Journal of Sound and Vibration 329 (2010) 2114–2126

Contents lists available at ScienceDirect

Journal of Sound and Vibration

journal homepage: www.elsevier.com/locate/jsvi

Elastic constants of a plate from impact-echo resonance and Rayleigh wave velocity

R. Medina *, A. Bayón

Departamento de Física Aplicada a los Recursos Naturales, ETSI Minas, Universidad Politécnica de Madrid, Ríos Rosas 21, 28003 Madrid, Spain

ARTICLE INFO

Article history:
Received 16 March 2009
Received in revised form
17 December 2009
Accepted 21 December 2009
Handling Editor: A.V. Metrikine
Available online 18 January 2010

ABSTRACT

A new method is proposed for calculating the dynamic elastic constants of an isotropic plate from measurements of the impact-echo resonance and Rayleigh wave velocity. Poisson's ratio is shown to be a single-valued function of the ratio between thickness frequency and Rayleigh wave velocity. This dependence is derived theoretically from the condition of resonance at the minimum frequency of the first-order symmetric Lamb mode. A finite element model is developed to determine how this frequency varies with Poisson's ratio. The results obtained by modal analysis and the power-spectral density technique are in good agreement with those calculated as the solution of the S1 Lamb mode equation. The method is verified by impact-echo tests on concrete and methacrylate plates. A laser interferometer is used to detect the vibration. Thickness frequencies are accurately identified by applying the multicross-spectral density to the signals detected at several points close to the impact point. In a separate experiment, Rayleigh waves are generated by the mediator technique. The wave velocities are determined from the arrival times of the surface wave at several points. Finally, the main sources of uncertainty are evaluated.

1. Introduction

Dynamic elastic constants are usually determined by measuring ultrasonic wave velocities or resonance frequencies in specimens of a convenient geometric shape, such as a cylinder or parallelepiped [1–3]. In general, the equations used to calculate elastic constants from wave velocities are valid for homogeneous and linearly elastic materials. Although concrete materials are not homogeneous, these equations can still be used if the wavelength of the elastic wave is much longer than the aggregates.

Several approaches have been proposed for calculating the dynamic elastic moduli of concrete materials from wave velocities. Quixian and Bungey [4] placed two conventional *P*-wave transducers on the surface of a sample to measure both longitudinal and Rayleigh wave velocities from the arrival of the wavefront. Wu et al. [5] measured the same velocities using transient elastic waves generated by a steel ball impact. In a later work [6], the procedure was improved and applied to a concrete plate using horizontally polarized transducers. Popovics et al. [7] presented a very accurate method of determining both wave velocities simultaneously from one-sided measurements. The arrival time of the first disturbance is corrected for pulse dispersion, enabling a more accurate determination of the *P*-wave arrival time. Measurements of the Rayleigh wave velocity and the normal-to-longitudinal amplitude ratio [8] can also be used as input data in the calculation of elastic constants. Surface waves are more easily identified than bulk waves, since they propagate with less attenuation.

* Corresponding author. Tel.: +34 913363240; fax: +34 913366952.
E-mail address: rafael.medina@upm.es (R. Medina).

0022-460X/$ - see front matter © 2009 Elsevier Ltd. All rights reserved.
doi:10.1016/j.jsv.2009.12.026

Another non-destructive technique, mainly used in the evaluation of concrete and masonry structures, is the impact-echo method [9]. Transient stress waves are generated by a short-duration mechanical impact, and a transducer located close to the impact point is used to detect the wavefront. After transforming the transducer signal into the frequency domain, significant peaks in the spectrum can be used to evaluate the integrity of the structure, determine the location of flaws, or measure its thickness [10,11]. Undesirable peaks in the spectrum due to interference from reflected waves can be reduced by various signal processing techniques, for example by calculating the multicross-spectral density [12]. In plate-like structures, the impact-echo response is dominated by reflections between the boundary surfaces, so the frequency spectrum will have a strong peak at the so-called thickness frequency (f_{t1}). The fundamental equation describing impact-echo response in a solid plate [9] is

$$f_{t1} = \frac{\beta v_P}{2h}, \tag{1}$$

where v_P corresponds to the velocity of the *P*-wave, h denotes the plate thickness, and β is a geometric correction factor equal to 0.96 for a concrete plate. Gibson and Popovics [13] established the theoretical basis for the correction factor β. Using guided wave theory, they proved that the impact-echo resonance corresponds to the point of zero group velocity at the frequency minimum of the first-order symmetric (S1) Lamb mode.

This paper investigates a different application of the impact-echo method: the thickness frequency is used to calculate the elastic constants of an isotropic plate. While other studies refer mainly to concrete, this paper deals also with other materials with different values of Poisson's ratio. To obtain an accurate thickness frequency, the high-amplitude Rayleigh wave generated by the impact should be removed [14]. However, before filtering out the Rayleigh wave, the detected signals at two points could be used to obtain the Rayleigh wave velocity. Therefore, in a single test with two detectors, both the thickness frequency and the Rayleigh wave velocity can be obtained.

In sum, this work proposes a new method for calculating the elastic constants of a plate from measurements of the thickness frequency and Rayleigh wave velocity. The signals detected in an impact-echo test are processed using the multicross-spectral density technique, in order to more accurately determine the thickness frequency. The Rayleigh wave velocity is obtained in a different experiment from the arrival times of a pulse at several aligned points. A broad-bandwidth laser interferometer is used to detect the vibrations, requiring no mechanical interaction with the sample. The method is experimentally tested and the main sources of uncertainty are evaluated.

2. Theoretical background

The classic problem of Lamb wave propagation in a traction-free, homogeneous and isotropic plate has been addressed by many researchers [15,16]. The solutions are a combination of travelling waves along the direction of the plate and standing waves in the transverse direction. The case of Lamb wave resonance at the minimum frequency of the first-order symmetric mode (S1) has been shown [13] to correspond to the impact-echo resonance. Since at this frequency the group velocity is zero, this mode tends to dominate the transient response of a plate to a mechanical impact when the detector is located near the impact area.

For the sake of simplicity in the calculation, let us define the dimensionless frequency Ω and the dimensionless wave number ξ as

$$\Omega = \frac{2hf}{v_S}, \quad \xi = \frac{hk}{\pi}, \tag{2}$$

where f denotes the frequency in Hz, v_S is the shear wave velocity, and k is the wave number. The equation relating the dimensionless frequency to the dimensionless wave number for symmetric Lamb modes is [15]

$$0 = \frac{\tan\left(\sqrt{(\Omega^2-\xi^2)}\cdot\pi/2\right)}{\tan(\sqrt{(\Omega^2/\kappa^2-\xi^2)}\cdot\pi/2)} + \frac{4\xi^2\sqrt{(\Omega^2/\kappa^2-\xi^2)}\sqrt{(\Omega^2-\xi^2)}}{(\Omega^2-2\xi^2)^2}. \tag{3}$$

The material constant $\kappa = v_P/v_S$, the ratio of longitudinal velocity v_P to shear velocity v_S, may be expressed in terms of Poisson's ratio v as

$$\kappa = \sqrt{\frac{2(1-v)}{1-2v}}. \tag{4}$$

The solution to Eq. (3) gives the dispersion relation for symmetric modes, but can only be obtained by numerical methods. In this work, Maple (*R*) is used to find the roots of Eq. (3). Fig. 1 shows the dispersion curves of the three lowest symmetric modes (S0, S1, S2), assuming a Poisson's ratio of 0.2. Note that the zero group velocity point lies at the frequency minimum of the first-order symmetric Lamb mode S1. The corresponding dimensionless frequency is denoted by $\Omega_{S1\,min}$. To investigate the dependence of such modes on Poisson's ratio, we created plots similar to Fig. 1 for Poisson's ratios ranging from 0.10 to 0.44. Fig. 2 shows the results for mode S1. The relationship between $\Omega_{S1\,min}$ and v is accurately obtained from the minima shown in Fig. 2 (solution to Eq. (3)), and is plotted in Fig. 3 as the curve labeled *analytical*. According to the

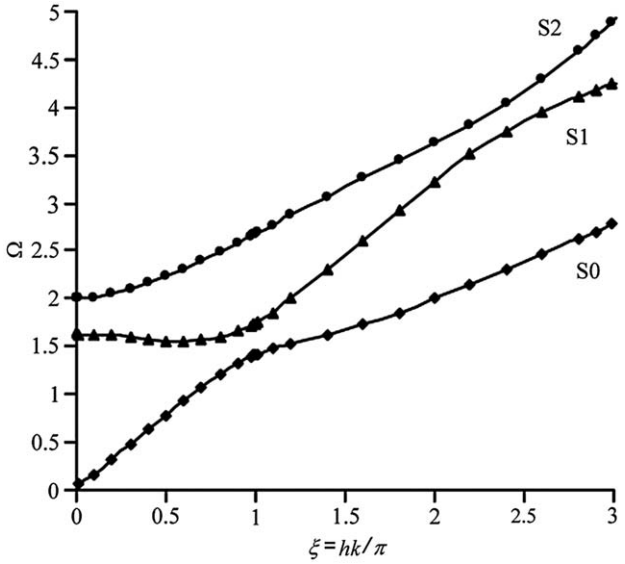

Fig. 1. Dispersion curves for the three lowest-order symmetrical Lamb waves, for a Poisson's ratio of 0.2.

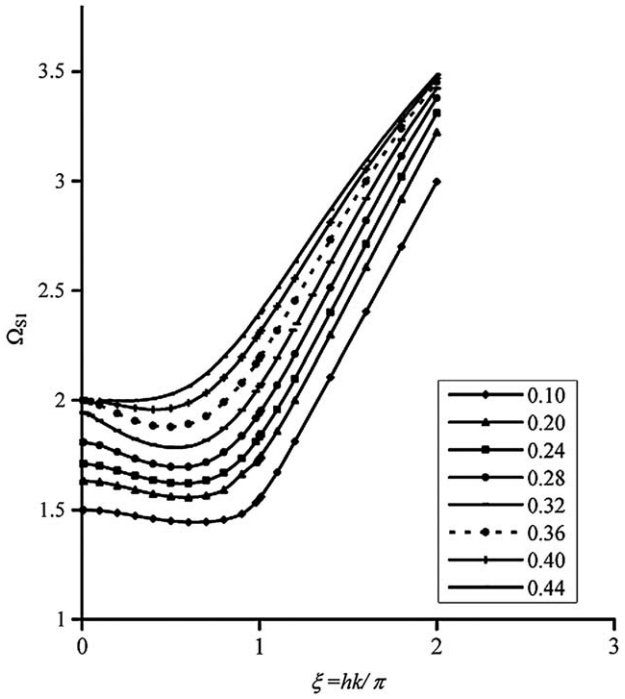

Fig. 2. Dispersion curves for the S1 Lamb wave only, for various Poisson's ratios from 0.10 to 0.44.

definition of Ω and the relationship between $\Omega_{S1\,min}$ and the thickness frequency f_{t1}, $\Omega_{S1\,min}$ can be expressed as $\Omega_{S1\,min}=2hf_{t1}/v_S$.

The exact value of the ratio between Rayleigh wave velocities v_R and v_S, $\eta=(v_R/v_S)^2$, can be calculated from the following equation:

$$\eta^3-8\eta^2+8\eta\left(3-2\frac{v_S^2}{v_P^2}\right)-16\left(1-\frac{v_S^2}{v_P^2}\right)=0. \tag{5}$$

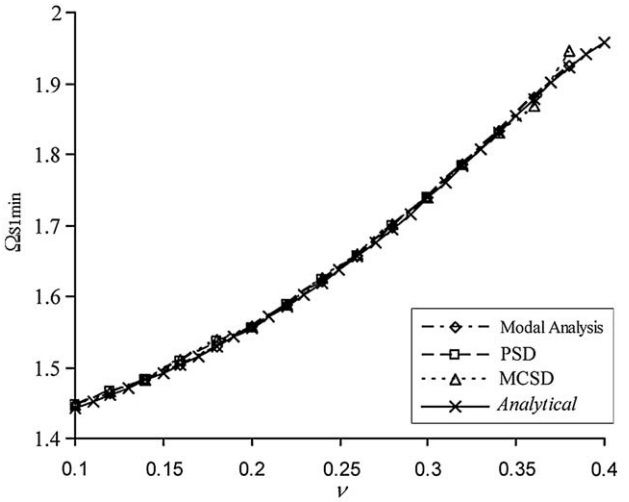

Fig. 3. Minimum frequency $\Omega_{S1\,min}$ of the first-order symmetric Lamb mode in terms of Poisson's ratio. The results are obtained by solving the analytical expression for the S1 Lamb mode (*analytical*), by modal analysis of a finite element model (FEM), by identifying the thickness frequency peak in the power spectral density (PSD), and by combining several independent PSDs into the multicross-spectral density (MCSD).

Since the ratio v_P/v_S depends only on ν, so does the ratio v_R/v_S, i.e., $v_R/v_S=f(\nu)$. A good approximation is given by [15]

$$\frac{v_R}{v_S}\approx\frac{0.862+1.14\nu}{1+\nu}. \tag{6}$$

From the expressions for $\Omega_{S1\,min}$ and $v_R/v_S=f(\nu)$, and the approximate solution to Eq. (5), it follows that

$$\Omega_{S1\,min}=\frac{2hf_{t1}}{v_S}=\frac{2hf_{t1}}{v_R}f(\nu)\approx\frac{2hf_{t1}}{v_R}\frac{0.862+1.14\nu}{1+\nu}. \tag{7}$$

$\Omega_{S1\,min}$ is indeed a function of ν, as shown in Fig. 3. Therefore, the relationship between hf_{t1}/v_R and Poisson's ratio can be established from Eq. (7). To increase the accuracy, the function $v_R/v_S=f(\nu)$ (the solution to Eq. (5)) is also accurately determined and will be included in the calculations performed in Section 4.

As mentioned earlier, the impact-echo method is based on the detection of the thickness frequency $f_{t1}=\beta(v_P/2h)$. Gibson and Popovics [13] showed that the empirical correction factor β is dependent on Poisson's ratio. Their study included plates with ν values ranging from 0.15 to 0.26.

An analytical expression giving the dependence of β on ν can be obtained in a straightforward manner. From the definition of $\Omega_{S1\,min}$ and Eq. (4), the thickness frequency takes the form

$$f_{t1}=\Omega_{S1\,min}(\nu)\frac{v_S}{2h}=\Omega_{S1\,min}(\nu)\sqrt{\frac{1-2\nu}{2(1-\nu)}}\frac{v_P}{2h}. \tag{8}$$

It follows from Eqs. (8) and (1) that the coefficient β can be analytically expressed as

$$\beta(\nu)=\Omega_{S1\,min}(\nu)\sqrt{\frac{1-2\nu}{2(1-\nu)}}. \tag{9}$$

This equation yields values of β in terms of ν on the condition that $\Omega_{S1\,min}(\nu)$ is known. Fig. 4 plots this relationship as the curve labeled *analytical*.

3. FEM analysis

The purpose of this section is to study by FEM analysis the dependence of the zero group velocity (ZGV) frequency in the first-order symmetric mode, $\Omega_{S1\,min}$, on ν for real (non-infinite) plates. The frequency associated with the thickness is calculated by modal analysis and by the power spectral density technique. The two results are compared to one another and to the *analytical* solution obtained in Section 2 for infinite plates. The range of ν for which the thickness frequency dominates the frequency response is also determined.

Modeling is performed with the finite element model software Ansys (*R*) 11.0 and a Pentium (*R*) 4 computer. In order to simulate a 3D plate with sufficient mesh refinement and a feasible computation time, we create a 2D model using rectangular quadratic axisymmetric elements.

Modal analysis obtains the frequency of vibration from the deformed shape corresponding to the thickness mode [13]. Since the generated wave amplitude increases greatly as the ZGV frequency is approached, the power spectral density

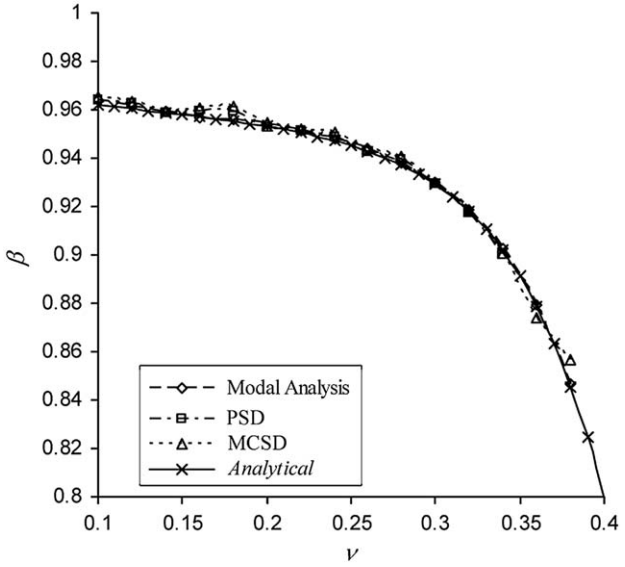

Fig. 4. The geometrical coefficient β used in the impact-echo method versus Poisson's ratio. β is calculated from the values of $\Omega_{S1\,min}$.

(PSD) is also proposed here to determine this frequency in a real plate. An impact is applied to the surface of the plate and the PSD response is calculated using the Ansys RPSD command. While modal analysis of the FEM requires the shape to be known, the PSD technique yields a direct and accurate estimate of the ZGV frequency without previous identification of the corresponding mode shape. The power spectral density analysis also determines the degree of excitation of the $\Omega_{S1\,min}$ mode in a plate subjected to an impact.

To improve the results, the PSD signal, $P_i(\omega)$, is recorded at various distances from the impact point, all points being within the area of relevance for an impact-echo test. Then they are combined to obtain the multicross-spectral density (MCSD) [12]. The MCSD signal $S_n(\omega)$ can be written as

$$S_n(\omega) = \prod_{i=1}^{n} P_i(\omega). \tag{10}$$

It is expected that only frequencies with high amplitudes in all spectra (the thickness frequency) will have a significant amplitude in S_n. The ZGV frequency is accurately calculated from the result given by Eq. (10) for the thickness frequency, $\Omega_{S1\,min} = 2hf_{t1}/v_S$.

The plate is modeled as having finite lateral dimensions and no support. Its material properties are assumed to be homogeneous and linear-elastic, which is the case for low-strain, low-frequency deformations in concrete. Various geometries L/h are studied, where L is the lateral dimension (the radius of the plate) and h is its thickness. A convergence analysis is carried out to accurately determine the grid spacing required when this ratio is large: in practice, the thickness frequency stabilizes once the element size has decreased to $\Delta x = 0.6h/20$.

We also determine the minimum admissible value of L/h. A FEM with $E = 40\,\text{GPa}$, $\nu = 0.2$, $\rho = 2400\,\text{kg m}^{-3}$, and $L = 2.5\,\text{m}$ is used to study the dependence of ZGV frequency on thickness values ranging from $h = 0.1$ to $0.6\,\text{m}$. Optimum results are obtained for $L/h > 6$; in this range the dimensionless ZGV frequency is independent of the thickness. Its value is $\Omega_{S1\,min} = 1.5588 \pm 0.0013$, similar to the *analytical* result (for a plate of infinite length) of $\Omega_{S1\,min} = 1.5563$.

The dependence of ZGV frequency on Poisson's ratio is studied using a circular plate with $E = 40\,\text{GPa}$, $\rho = 2400\,\text{kg m}^{-3}$, $L = 2.5\,\text{m}$, and $h = 0.15\,\text{m}$. Poisson's ratio is varied from 0.10 to 0.38, with an interval of 0.02. (For values of ν outside this interval, the thickness frequency is difficult to identify.) In this analysis $\Omega_{S1\,min}$ is calculated by three methods: modal analysis (deformed shape), the Ansys-PSD, and the MCSD (Eq. (10)). An example of the deformed shape corresponding to the thickness frequency is shown in Fig. 5(a), for $\nu = 0.24$. The mode is a symmetric resonance with large deformations in the central area, the zone of relevance to the impact-echo test. Figs. 5(b) and (c) show the PSD and the MCSD results, respectively. In the latter, only one peak appears in the spectrum. The frequencies obtained are $f = 14\,004\,\text{Hz}$ from the deformed shape study, $f = 14\,020\,\text{Hz}$ from the PSD, and $f = 14\,047\,\text{Hz}$ from the MCSD. The corresponding values of $\Omega_{S1\,min}$ differ from the *analytical* solution by less than 0.38 percent. Fig. 3 shows the variation of $\Omega_{S1\,min}$ with ν for all three methods, including the *analytical* solution for comparison.

Fig. 4 shows the variation of β with ν. This coefficient decreases with Poisson's ratio, an effect which is especially significant for large values of ν. The dimensionless ZGV frequency, on the other hand, increases with Poisson's ratio.

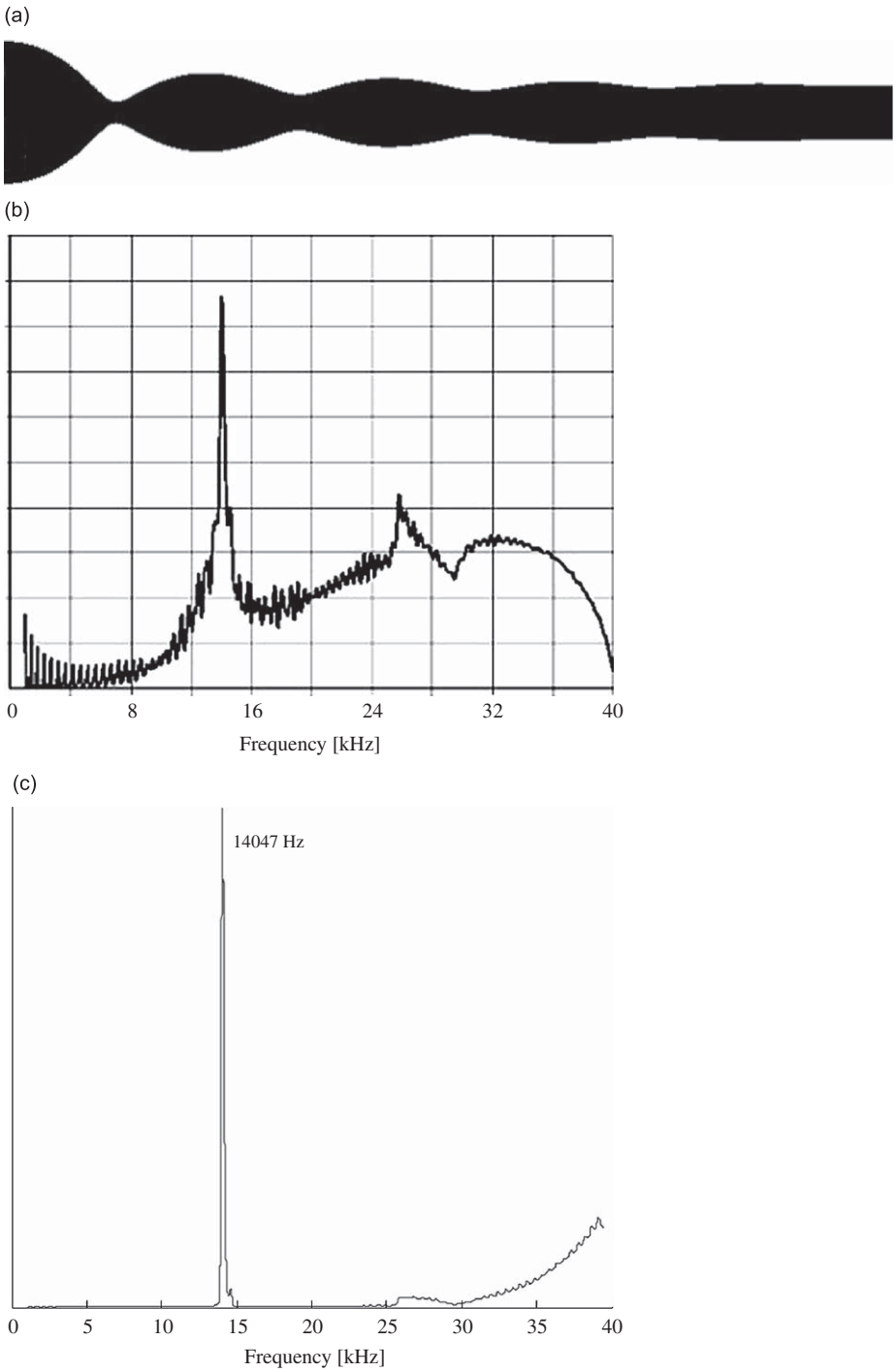

Fig. 5. Results obtained by FEM analysis for the zero-group-velocity (ZGV) frequency of the first-order symmetric mode: (a) the mode shape, (b) the power spectral density (PSD), and (c) the multicross-spectral density (MCSD).

The values obtained for $\Omega_{S1\,min}$ under all three methods are similar to the *analytical* solution, as shown in Fig. 3. These numerical results prove that the *analytical* solution for the ZGV frequency of an infinite plate can correctly characterize real (non-infinite) plates. Our PSD analysis shows that the thickness mode is most easily excited in the interval $0.10 < v < 0.38$. For other values of v, the thickness frequency does not dominate the spectrum and is therefore difficult to identify. Characterization of materials based on the results of an impact-echo test can therefore be extended to other materials, provided their Poisson's ratios lie within the aforementioned interval.

4. Method for calculation of the elastic constants

The theoretical study of Section 2 shows that $\Omega_{S1\,min}$ is a single-valued function of ν. Conversely, a given value of $\Omega_{S1\,min}$ determines ν for the plate under examination. In light of Eq. (7), and given that the magnitudes h, f_{t1}, and v_R can be measured, we introduce the dimensionless parameter $W = hf_{t1}/v_R$. W can be expressed in terms of Poisson's ratio as

$$W = \frac{hf_{t1}}{v_R} = \frac{\Omega_{S1\,min}(\nu)}{2}\,\frac{1}{f(\nu)} \approx \frac{\Omega_{S1\,min}(\nu)}{2}\,\frac{1+\nu}{0.862+1.14\nu}. \tag{11}$$

Fig. 6 plots W versus ν, which is also a single-valued function. The second column of Table 1 provides the values of W, which are calculated from $\Omega_{S1\,min}$ and $f(\nu)$. The former is obtained in Section 2 from the solution of Eq. (3) for the frequency minimum of the first-order symmetric Lamb mode; the latter is given by Eq. (5) for each value of ν. Note that although the approximation of Eq. (11) is accurate enough for many applications, here the values of $f(\nu)$ are obtained by solving Eq. (5) instead. If h, f_{t1} and v_R are all known, W can be calculated and ν can be determined by interpolating the values in Table 1.

In order to fully characterize the elastic behavior of an isotropic plate, either Young's modulus or the shear modulus should also be calculated. Young's modulus E may be obtained by combining Eq. (1), the well-known relation of v_P to ν, and the dependence of β on ν established in Section 2:

$$E = \left(\frac{2hf_{t1}}{\beta}\right)^2 \frac{\rho\,(1+\nu)(1-2\nu)}{1-\nu}, \tag{12}$$

where ρ is the density of the material. The β values associated with each ν, calculated from Eq. (9), are also listed in Table 1. Nominally, Eq. (12) requires Poisson's ratio. However, since Table 1 shows the dependence of both ν and β on W, Eq. (12) can be expressed in terms of h, f_{t1}, ρ, and W. Therefore, ν is not needed to obtain E; either elastic constant can be calculated independently of the other.

The above study shows that the elastic constants of an isotropic plate can be calculated from measurements of the Rayleigh wave velocity and the thickness frequency. The thickness of the plate should be large compared with the wavelength of the surface wave. The thickness frequency is determined by an impact-echo test. The Rayleigh wave velocity could be determined in the same test by using two detectors. If only one detector is available, then two separate tests are required. The surface waves can be generated and detected by other means such as the wedge technique, a periodic array of transducers, and the mediator technique [17].

The quotient W and Table 1 can provide a value of ν through simple linear interpolation. Analogously, the value of β can be calculated from Table 1 provided either ν or W is known. Finally, Eq. (12) yields Young's modulus. Note that the density and thickness of the plate must be known.

5. Experimental procedure

In this section, we apply the methodology proposed above to isotropic plates of various materials. A laser interferometer is used to detect the vibration. Each sample is subjected to two experiments: one determines the thickness frequency by the impact-echo method, and the other generates Rayleigh waves by the "mediator technique" [17] to measure v_R.

Fig. 7(a) sketches the points of impact and detection for the first experiment. Elastic waves are generated by the brief impact of a steel ball moving perpendicular to the plate at its center. The steel ball is 3.20 mm in diameter. We estimate the

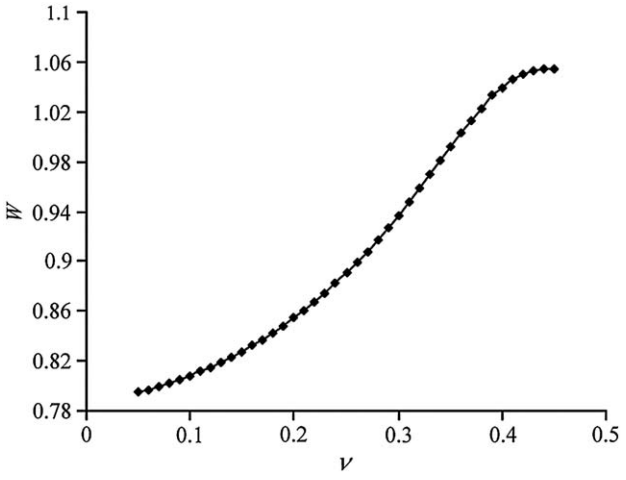

Fig. 6. The dimensionless parameter $W = hf_{t1}/v_R$ in terms of Poisson's ratio.

Table 1
Values of the dimensionless parameter W and coefficient β in terms of Poisson's ratio, as obtained from Lamb wave resonance $\Omega_{S1\,min}$ (*analytical* solution).

v	W	β	$\lvert\Delta v/\Delta W\rvert$	$\lvert\Delta\beta/\Delta v\rvert$
0.05	0.7946	0.9666	4.3478	0.1
0.06	0.7969	0.9656	4.1667	0.09
0.07	0.7993	0.9647	3.7037	0.09
0.08	0.8020	0.9638	3.5714	0.09
0.09	0.8048	0.9629	3.1250	0.08
0.1	0.8080	0.9621	3.0303	0.08
0.11	0.8113	0.9613	2.7778	0.08
0.12	0.8149	0.9605	2.5641	0.09
0.13	0.8188	0.9596	2.4390	0.08
0.14	0.8229	0.9588	2.2727	0.08
0.15	0.8273	0.9580	2.0833	0.09
0.16	0.8321	0.9571	2.0000	0.09
0.17	0.8371	0.9562	1.8519	0.1
0.18	0.8425	0.9552	1.7544	0.1
0.19	0.8482	0.9542	1.6667	0.12
0.2	0.8542	0.9530	1.5625	0.12
0.21	0.8606	0.9518	1.4706	0.14
0.22	0.8674	0.9504	1.3889	0.15
0.23	0.8746	0.9489	1.2987	0.17
0.24	0.8823	0.9472	1.2500	0.2
0.25	0.8903	0.9452	1.1765	0.23
0.26	0.8988	0.9429	1.1236	0.27
0.27	0.9077	0.9402	1.0638	0.31
0.28	0.9171	0.9371	1.0204	0.37
0.29	0.9269	0.9334	0.9804	0.43
0.3	0.9371	0.9291	0.9434	0.52
0.31	0.9477	0.9239	0.9174	0.61
0.32	0.9586	0.9178	0.9009	0.73
0.33	0.9697	0.9105	0.8929	0.88
0.34	0.9809	0.9017	0.9009	1.05
0.35	0.9920	0.8912	0.9091	1.26
0.36	1.0030	0.8786	0.9709	1.51
0.37	1.0133	0.8635	1.0309	1.79
0.38	1.0230	0.8456	0.9709	2.12
0.39	1.0333	0.8244	1.6949	2.49
0.4	1.0392	0.7995	1.6393	2.9
0.41	1.0453	0.7705	2.2222	3.36
0.42	1.0498	0.7369	3.4483	3.87
0.43	1.0527	0.6982	7.6923	4.43

The slopes $\lvert\Delta v/\Delta W\rvert$ and $\lvert\Delta\beta/\Delta v\rvert$ are also listed.

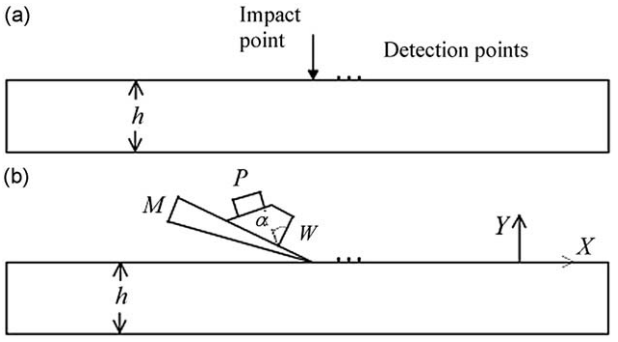

Fig. 7. (a) Experimental layout to determine the thickness frequency by the impact-echo method. (b) Sketch illustrating the mediator technique of generating surface waves and the detection points.

impact duration to be 13.7 μs, and expect to detect thickness frequencies up to 90 kHz. A laser Doppler vibrometer (Polytec OFV-5000) with a VD-06 velocity decoder is used to detect the out-of-plane velocity component at several locations. The laser interferometer has a frequency range of 0−350 kHz and a velocity range of 2 mm s^{-1}/V. No surface preparation is required. The detection points are arranged at various distances from the impact point, from 0.2 h to 0.8 h. The signals are digitized by an oscilloscope (Tektronik TDS5032B).

The fast Fourier transform (FFT) of the detected signal is expected to show a significant peak at the thickness frequency. However, the spectrum also contains undesirable peaks associated with low-frequency natural modes and interference from reflected waves. Some of these have very large amplitudes, and their presence in the spectrum would make the thickness frequency peak more difficult to identify. The duration of the recorded signal should be long enough to detect multiple reflections between the upper and lower surfaces of the plate, but short enough to prevent the detection of vibration modes whose amplitudes are large relative to the thickness frequency. Thus, in order to determine the thickness frequency with great accuracy, the recorded signals are first processed according to a procedure described in [12]. Firstly, a rectangular window is applied to remove Rayleigh waves from the signal and increase the signal-to-noise ratio of the frequency spectrum. Secondly, the multicross-spectral density is calculated. This technique combines the spectra of signals recorded at various locations, reducing the amplitude of undesired peaks associated with interference between the various waves. The procedure is similar to that described in Section 3 for the PSD response (Eq. (10)).

The second experiment measures the Rayleigh wave velocity. Fig. 7(b) illustrates the mediator technique of generating surface waves [17], and also indicates the detection points. A *P*-wave transducer (0.5 MHz) is set on the sloping surface of a wedge at the critical angle α which allows a Rayleigh wave to be generated on the surface of the mediator *M*. The generated surface wave is optimal when the angle of incidence is $\alpha = \sin^{-1}(v_{PW}/v_{RM})$, where v_{PW} is the *P*-wave velocity in the wedge and v_{RM} is the Rayleigh wave velocity in the mediator. Since v_{PW} must be smaller than v_{RM}, the wedge is made of methacrylate ($v_P = 2730\,\mathrm{m\,s^{-1}}$) and the mediator is made of aluminium ($v_R = 2888\,\mathrm{m\,s^{-1}}$). The angle α is therefore 71°. The generated wave travels first along the wedge, then along the mediator, then impinges on the plate. The advantage of this technique is that a sharp-tipped mediator can generate Rayleigh waves even in materials with low surface wave velocities. The same method is applied in all our experiments, regardless of the material of the sample. The amplitudes of the generated Rayleigh waves are very low, but sufficiently large to detect arrival times (albeit with difficulty). The Rayleigh waves are detected by means of a laser speckle heterodyne interferometer (Ultra-Optec OP35-I/O) [18]. Both normal and longitudinal components of the displacement can be detected at the same point, in sequential measurements.

In a preliminary experiment Rayleigh waves were generated on the surface of an aluminium plate, first by the wedge technique and then by the mediator technique. For the first measurement, the methacrylate wedge was directly adhered to the aluminium sample. The normal and longitudinal components of the Rayleigh wave were detected with the I/O interferometer. In the second measurement, only the normal component of the surface wave could be detected. The velocity of the wave was calculated from arrival times in both cases. The results obtained for the velocity were in good agreement. This experiment shows that Rayleigh waves are mainly generated using the mediator technique. The spot of light on the surface is about 20 μm in diameter. The wavelength of the Rayleigh wave should be large compared to the diameter of the illuminated zone, so that the detection can be regarded as "point-like".

As shown in Fig. 7(b), we detected the normal component of the Rayleigh wave with the interferometer at several aligned points. The arrival time of the surface wave is taken as the arrival time of the first peak. The set of times t_i taken for the wave to arrive at coordinates x_i are used in a linear regression to determine the velocity. The signal detected at each point is averaged to improve the signal-to-noise ratio.

6. Experimental results

The proposed method is applied to sample plates of two different materials: methacrylate and concrete. The sample dimensions are detailed in Table 2. The width-to-thickness ratios are approximately 15 and 7 for methacrylate and concrete, respectively. The concrete sample was mixed and cast in our laboratory.

The signals generated by the impact are detected at several points on the surface, at various distances from the impact point. These distances range from 5 to 20 mm for the methacrylate plate, and from 16 to 32 mm for the concrete sample. The sampling intervals used to record the displacement waveform are 400 and 800 ns for methacrylate and concrete, respectively. As an example, Fig. 8 shows the displacement waveform recorded by the laser interferometer at a single point on the methacrylate sample. The plot shows a Rayleigh wave with large amplitude and multiple reflections between the parallel surfaces of the plate. As mentioned in Section 5, a rectangular window of 4096 datapoints is applied to remove the Rayleigh wave. The start of the window is delayed at each point by the time required for the Rayleigh wave to travel to that point. We then apply the fast Fourier transform (FFT) to each time series. With 4096 points, the resolutions of the frequency spectra are 610 Hz for the methacrylate sample and 305 Hz for the concrete sample.

Figs. 9 and 10 show the multicross-spectral density functions obtained for the methacrylate and concrete samples, respectively. The energy of the impact is too low to excite flexural modes. For the concrete sample, a single major peak

Table 2
Geometrical dimensions of the methacrylate and concrete plates: length *l*, width *w*, thickness *h*, and density ρ.

Sample	l (cm)	w (cm)	h (cm)	ρ (kg m^{-3})	f_{t1} (Hz)	v_R (m s^{-1})
Methacrylate	40.0	40.0	2.520	1182	49088	1286
Concrete	60.0	60.0	8.1	2191	20214	1905

The experimental results for the impact-echo resonance f_{t1} and Rayleigh wave velocity v_R of the plates are also included.

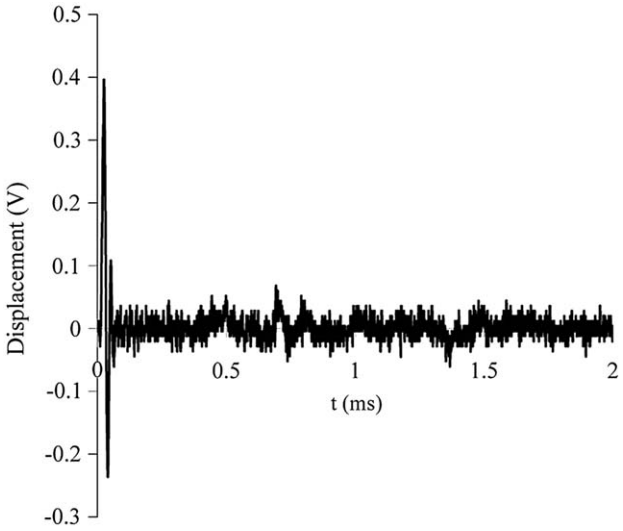

Fig. 8. Displacement waveform from an impact-echo test at a point on the methacrylate plate.

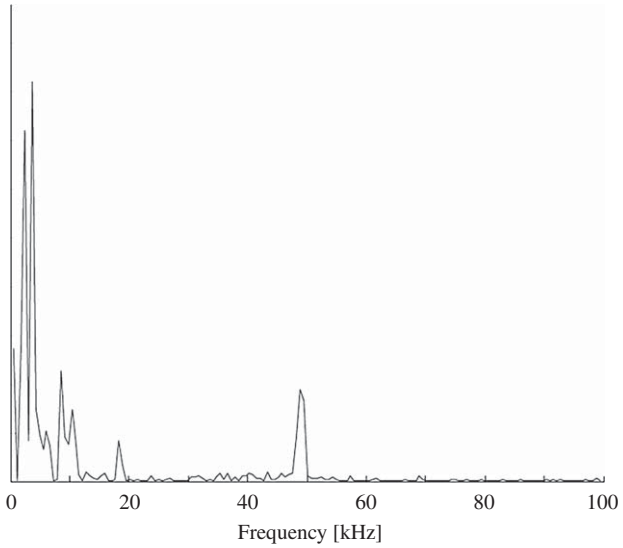

Fig. 9. Multicross-spectral density for the methacrylate sample.

appears at 20 141 Hz. The methacrylate sample has a more complicated MCSD, with a large peak at 48 828 Hz accompanied by lateral peaks at 48 217 and 49 438 Hz. The actual thickness frequency is therefore expected to lie between these values. The resolution cannot be improved further; a longer duration would introduce high-amplitude natural frequencies into the spectrum, decreasing the signal-to-noise ratio of the thickness frequency peaks. The thickness frequencies f_{t1} reported in Table 2 are weighted averages of the frequency at maximum amplitude and the frequencies of the two adjacent values on either side of that peak.

Table 2 also reports Rayleigh wave velocities obtained following the methodology described in Section 5. The sample is mounted on a translation stage with a precision of 0.01 mm. The arrival time of the wave at several positions is measured with the I/O interferometer. The velocity is the slope of the least-squares linear fit to the set of distances x (mm) and arrival times t (μs). For the methacrylate plate, the best-fit line through four points is $x = 1285.7t$ (the correlation coefficient is $r = 0.9999$). Fig. 11 shows the normal displacements detected at a single point. The size of the concrete sample makes it impossible to use the translation stage, so the I/O interferometer cannot be used to detect Rayleigh waves in this experiment. Instead, the laser vibrometer is mounted on the translation stage and used to detect the arrival of the wave at three locations. The resulting slope is $1905\,\mathrm{m\,s^{-1}}$ ($r = 1$).

Table 3 shows the ν and E values obtained by applying the proposed method to the samples. From $W = hf_{t1}/v_R$, linear interpolations of Table 1 give Poisson's ratio ν and β. Note that β can also be calculated from the value of ν, using the

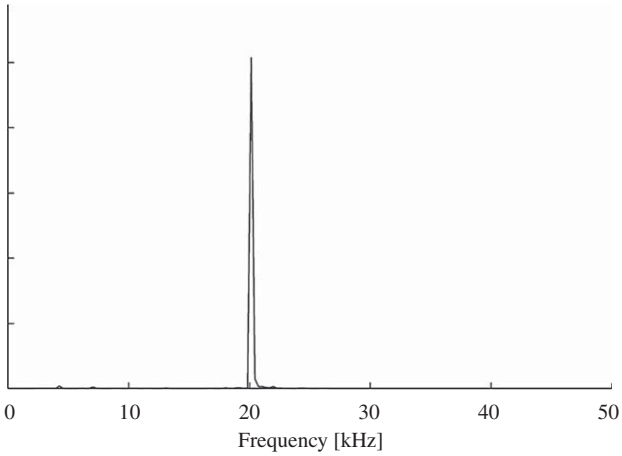

Fig. 10. Multicross-spectral density for the concrete sample.

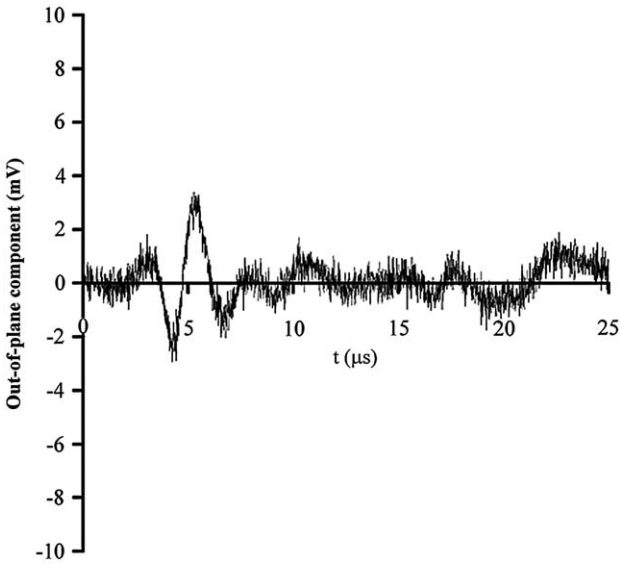

Fig. 11. Normal component of the Rayleigh wave at a point on the methacrylate sample.

Table 3
Values of the dimensionless parameter W and coefficient β, along with the calculated values of Poisson's ratio v and Young's modulus E for the samples tested.

Sample	W	v	β	E (GPa)
Methacrylate	0.9619	0.3230	0.9156	5.97
Concrete	0.8595	0.2083	0.9520	23.08

function $\beta(v)$ shown in Table 1. Eq. (12) then yields the value of E. A graphical solution can be found from Figs. 4 and 6; no tables are required.

For purposes of comparison, the dynamic elastic constants of these samples are calculated based on measurements of the bulk wave velocities v_P and v_S. Conventional ultrasonic measurements are performed through the thickness of the samples to obtain these velocities. For the methacrylate sample, this method gives E and v values of 6.00 GPa and 0.3237, respectively. The differences between these results and those shown in Table 3 are 0.2 and 0.5 percent, respectively. For the concrete sample, the bulk velocities estimated give $E = 26.11$ GPa and $v = 0.1982$. Compared to our method, the relative differences are 10.7 and 5 percent, respectively.

7. Estimation of the uncertainties of the method

The uncertainty U of an indirect measurement is estimated by taking the partial derivative of the function relating the result y to the directly measurements x_i [19]: $U_y = \sum |\partial y/\partial x_i| U_{x_i}$. Here we assume that the uncertainty in direct measurements U_{x_i} is only due to the lack of resolution of the apparatus. The uncertainties obtained for ν and E are not based on a statistical analysis of repeated experiments, so should be considered minimal estimates.

The uncertainty in the dimensionless parameter W, U_W, is calculated from those of the thickness (U_h), the frequency ($U_{f_{t1}}$), and an indirect measurement of ν_R (U_{ν_R}). U_W can be written as

$$U_W = \left|\frac{\partial W}{\partial h}\right| U_h + \left|\frac{\partial W}{\partial f_{t1}}\right| U_{f_{t1}} + \left|\frac{\partial W}{\partial \nu_R}\right| U_{\nu_R}. \tag{13}$$

The thickness of the methacrylate sample is measured with a caliper ($U_h = 0.05$ mm); the concrete is measured with a ruler ($U_h = 1$ mm). Based on the sampling frequency and the number of data points, the uncertainties of frequencies obtained in the FFT analysis are $U_{f_{t1}} = 610$ Hz for the methacrylate sample and $U_{f_{t1}} = 305$ Hz for the concrete plate. The uncertainty of the Rayleigh wave velocity is estimated by applying the same methodology, propagating the uncertainties on the distances and the elapsed times. As a translational mechanism is used to adjust the sample, $U_x = 0.01$ mm. In the measurement of the time elapsed, it is estimated that $U_t = 0.01$ μs.

Poisson's ratio ν is calculated from its dependence on W, which is accurately established in Table 1. Therefore, the uncertainty of ν can be expressed as

$$U_\nu = \left|\frac{\partial \nu}{\partial W}\right| U_W \approx \left|\frac{\Delta \nu}{\Delta W}\right| U_W. \tag{14}$$

In order to calculate ν with high precision, the partial derivative of ν with respect to W should be as small as possible. However, this derivative depends on the value of ν. The fourth column of Table 1 lists the absolute value of the slope $|\Delta\nu/\Delta W|$. The smallest (approximately constant) slopes occur in the interval $0.27 < \nu < 0.38$. For values of ν smaller than 0.27, the slope increases gradually down to a Poisson's ratio of approximately 0.14, below which the variation is more pronounced. For Poisson's ratios greater than approximately 0.42, the slope increases rapidly, indicating that any calculation of Poisson's ratio in this range will be highly uncertain.

From Eq. (12), it follows that the uncertainty of E is given by

$$U_E = \left|\frac{\partial E}{\partial h}\right| U_h + \left|\frac{\partial E}{\partial f_{t1}}\right| U_{f_{t1}} + \left|\frac{\partial E}{\partial \beta}\right| U_\beta + \left|\frac{\partial E}{\partial \rho}\right| U_\rho + \left|\frac{\partial E}{\partial \nu}\right| U_\nu, \tag{15}$$

where β is calculated by linear interpolation in Table 1 and U_β is determined by the same procedure followed for U_ν. By taking β as a function of ν, U_β can be estimated as $U_\beta \approx |\Delta\beta/\Delta\nu| U_\nu$. The fifth column of Table 1 lists results for the slope $|\Delta\beta/\Delta\nu|$. The slopes are small and roughly constant for values of ν smaller than 0.2. As with Poisson's ratio, the slope increases sharply for Poisson's ratios greater than approximately 0.4. In this range the uncertainties are large, and the proposed method is not recommended.

Finally, after substituting U_W given by Eq. (13) into Eq. (14), we obtain the overall uncertainties on our parameters of interest. For the methacrylate sample, we find $U_\nu = 0.0017 + 0.0108 + 0.0024 = 0.0149$. The first term corresponds to U_h, the second to U_{ft1}, and the third to U_{ν_R}. The relative uncertainty is $U_\nu/\nu = 4.6$ percent. Most of this comes from U_{ft1}, which is a relative uncertainty of (72.5 percent). To improve the precision of the measurement, this uncertainty must be decreased. For the concrete sample, $U_\nu = 0.0166 + 0.0203 + 0.0062 = 0.0431$ and the relative uncertainty is 20.7 percent. The main contribution to the uncertainty on ν is also U_{ft1} (47 percent). A larger value of U_ν is obtained for the concrete sample because this measurement is less sensitive to uncertainty in the thickness of the plate.

When Eq. (15) is applied to the indirect measurement of U_E, the result for the methacrylate sample is $U_E = 0.02 + 0.15 + 0.14 + 0.02 + 0.30 = 0.63$ GPa, and the relative uncertainty is $U_E/E = 10.6$ percent. The uncertainty in the measurement of ν accounts for 48 percent of U_E, while the thickness frequency accounts for 24 percent. The measurements of both ν and E can thus be improved by decreasing $U_{f_{t1}}$, i.e., by modifying the sampling parameters.

For the concrete sample, $U_E = 0.57 + 0.70 + 0.25 + 0.05 + 1.33 = 2.90$ GPa, the relative uncertainty being 12.6 percent. For this sample, a decrease in both U_ν and U_E can be accomplished by measuring the thickness with greater sensitivity and decreasing U_{ft1}.

If the uncertainty of f_{t1} were improved by prolonging the recording time, the amplitude of the natural frequencies would increase, possibly preventing detection of the thickness frequency peak. The solution would be to find a means of filtering out these low frequencies.

These uncertainty estimates are only valid for the specific materials and experimental set-up used in this research, but it is straightforward to extend the procedure to materials with similar values of ν.

8. Conclusions

This paper has described a new method for calculating the dynamic elastic constants of a finite plate. Poisson's ratio can be computed as a simple quotient of the impact-echo resonance and Rayleigh wave velocity, provided the thickness of the

plate is known. The dependence of Poisson's ratio on these two factors was derived independently from the S1 Lamb mode equation and a FEM analysis, the results being in good agreement. The geometric correction factor β, used in the impact-echo method, is also related to Poisson's ratio and permits calculation of Young's modulus.

Satisfactory results can be obtained for materials whose Poisson's ratios lie within the approximate interval 0.14–0.38. For lower and higher values, the partial derivatives of Poisson's ratio with respect to the aforementioned factors are very high, leading to results with high uncertainty. Within this interval the main source of uncertainty is the thickness frequency, which is limited by the low resolution of the spectra. Although a higher resolution can be achieved simply by increasing the recording time, large-amplitude natural frequency peaks will appear in the spectrum, possibly preventing detection of the thickness frequency peak. The thickness frequency peak can be more accurately identified by computing the multicross-spectral density of multiple signals detected in the impact-echo test.

The numerical results show that the thickness mode is highly excited for Poisson's ratios within the suggested interval (0.14–0.38). Experimental verification of the method is performed by testing concrete and methacrylate plates. Two separate tests were carried out on each plate: the impact-echo test to measure the thickness frequency, and another experiment to measure the velocity of Rayleigh waves. If two detectors were used, however, a single impact-echo test would be sufficient to determine the elastic constants of an isotropic plate.

Acknowledgments

This work has been partially supported by the Spanish Governmental "Plan Nacional de I+D+i 2004-2007" under Project no. BIA2004-07428-C02 of the "Programa Nacional de Construcción".

References

[1] C848-88(2006) "Standard Test Method for Young's Modulus, Shear Modulus, and Poisson's Ratio For Ceramic Whitewares by Resonance", C215-08 "Standard Test Method for Fundamental Transverse, Longitudinal, and Torsional Frequencies of Concrete Specimens", and other ASTM standards (American Society for Testing and Materials, Philadelphia, PA).
[2] P. Heyliger, A. Jilani, Elastic constants of isotropic cylinders using resonant ultrasound, *Journal of the Acoustical Society of America* (1993) 1482–1487.
[3] F.J. Nieves, F. Gascón, A. Bayón, Measurement of the dynamic elastic constants of short isotropic cylinders, *Journal of Sound and Vibration* 265 (2003) 917–933.
[4] L. Quixian, J.H. Bungey, Using compression wave ultrasonic transducers to measure the velocity of surface waves and hence determine dynamic modulus of elasticity for concrete, *Construction and Building Materials* 10 (4) (1996) 237–242.
[5] T.T. Wu, J.S. Fang, G.Y. Liu, M.K. Kuo, Determination of elastic constants of a concrete specimen using transient elastic waves, *Journal of the Acoustical Society of America* 98 (4) (1995) 2142–2148.
[6] D.T.T. Wu, J.S. Fang, A new method for measuring in situ concrete elastic constants using horizontally polarized conical transducers, *Journal of the Acoustical Society of America* 101 (1) (1997) 330–336.
[7] J.S. Popovics, W. Song, J.D. Achenbach, J.H. Lee, R.F. Andre, One-sided stress wave velocity measurement in concrete, *Journal of Engineering Mechanics* 124 (12) (1998) 1346–1353.
[8] A. Bayón, F. Gascón, F.J. Nieves, Estimation of dynamic elastic constants from the amplitude and velocity of Rayleigh waves, *Journal of the Acoustical Society of America* 117 (6) (2005) 3469–3477.
[9] M.J. Sansalone, W.B. Streett, *Impact-Echo: Nondestructive Evaluation of Concrete and Mansonry*, Bullbrier Press, Jersey Shore, PA, 1997.
[10] M. Sansalone, N.J. Carino, Transient impact response of plates containing flaws, *Journal of Research of the National Bureau of Standards* 92 (6) (1987) 369–381.
[11] C. Hsiao, C.C. Cheng, T. Liou, Y. Juang, Detecting flaws in concrete blocks using the impact-echo method, *NDT&E International* 41 (2008) 98–107.
[12] R. Medina, M. Garrido, Improving impact-echo method by using cross-spectral density, *Journal of Sound and Vibration* 304 (2007) 769–778.
[13] A. Gibson, J.S. Popovics, Lamb wave basis for impact-echo method analysis, *Journal of Engineering Mechanics* 131 (4) (2005) 438–443.
[14] O. Abraham, C. Léonard, P. Côte, B. Piwakowski, Time frequency analysis of impact-echo signals: numerical modelling and experimental validation, *ACI Materials Journal* 97 (6) (2000) 645–657.
[15] J.D. Achenbach, *Wave Propagation in Elastic Solids*, Elsevier Science Publishers B.V., Amsterdam, 1975.
[16] K.F. Graff, *Wave Motion in Elastic Solids*, Dover, New York, 1991.
[17] J.L. Rose, *Ultrasonic Waves in Solid Media*, Cambridge University Press, London, 1999.
[18] J.P. Monchalin, J.D. Aussel, R. Heon, C.K. Jen, A. Boundreault, R. Bernier, Measurements of in-plane and out-of-plane ultrasonic displacements by optical heterodyne interferometry, *Journal of Nondestructive Evaluation* 8 (1989) 121–132.
[19] J.R. Taylor, *An Introduction to Error Analysis*, University Science, Mill Valley, 1982.